Dielectric cavity QED between photonic crystals: An effective uniaxial medium approach

Ali Kamli[1] and M. Babiker[2]
[1]*Department of Physics, King Khalid University, Abha P.O. Box 9003, Saudi Arabia and Rochester Theory Center for Optical Science and Engineering, Department of Physics and Astronomy, University of Rochester, Rochester, New York 14627*
[2]*Department of Physics, University of York, Heslington, York Y010 5DD, United Kingdom*
(Received 15 February 2000; published 11 September 2000)

The spontaneous-emission rate is evaluated for dipole emitters situated in the thin slab region between two semi-infinite one-dimensionally periodic photonic crystals, a situation reminiscent of planar cavity laser structures. It is pointed out that the long-wavelength electromagnetic fields supported by such complex structures can be directly quantized provided that the pair of semi-infinite photonic crystals are treated within the effective-medium approach, in which each photonic crystal is represented by a truncated uniaxial medium whose dielectric tensor components are determinable in terms of layer thicknesses and dielectric functions of the individual photonic crystal components. The spontaneous-emission rate is evaluated for a dipole emitter situated in the slab region, and oscillating at a frequency resonant with one of the modes that are localized within the slab and exponentially decaying within the photonic crystals. Both symmetric and asymmetric structures are discussed. Interesting features are predicted when the variations of the adjustable parameters are examined, including suppression and enhancement of the spontaneous rate.

PACS number(s): 42.50.Dv, 42.50.Ct, 42.70.Qs

I. INTRODUCTION

It has been unambiguously established in cavity quantum electrodynamics (CQED) that the spontaneous rate of a point dipole emitter can be controlled at will by suitably tailoring the environment in which the dipole emitter is situated. Since the pioneering work of Purcell [1], much research has been carried out, especially recently, on the modification of the spontaneous rate and its practical consequences for dipoles immersed in various dielectric media and cavity structures of different shapes and sizes. The dielectric slab structure, in particular, has been the subject of investigation by many authors [2–6], but most treatments of this problem considered the simplest case in which the slab is sandwiched between two much thicker layers of isotropic media. There has also been little work done on the influence of possible frequency dependence [7] of the relevant dielectric functions in this three-layer structure.

In a parallel development, considerable work was done recently on electromagnetic modes guided within artificially fabricated ordered photonic crystal structures [8–11]. These structures can lead to the generation of efficient semiconductor laser sources, principally because they can act not only as efficient waveguides, but also provide the possibility of reducing, or maybe even completely suppressing, spontaneous emission. A particular configuration often encountered in planar cavity laser structures is that in which the dipole emitter is situated in the thin slab region between two semi-infinite one-dimensionally periodic photonic crystals [12]. We concentrate here on this configuration, because of its relevance to laser structures. We evaluate the spontaneous emission rate for this situation, and explore the factors that influence the suppression and enhancement of this rate.

Fortunately, the problem can be reduced to that of the three-layer slab structure mentioned above by invoking the effective-medium approach which has been successfully applied to the study of various electromagnetic excitations in layered structures [13–16]. The effective-medium approximation considered here pertains to any layer structure formed by the alternate periodic stacking of two types of layers of locally isotropic materials of thicknesses d_1 and d_2 with dielectric functions ε_1 and ε_2, one or both of which may be frequency dependent. This layer system is regarded as equivalent to a homogeneous uniaxial medium with a diagonal dielectric tensor containing two distinct components: one for propagation along the optical axis, and the second for propagation parallel to the interfaces. Once this approximation has been applied, one can deal with the quantization of the electromagnetic field modes of a homogeneous, but anisotropic medium which can then be made to form one of the sandwich layers in the slab structure under consideration involving two semi-infinite periodic photonic crystals. With the electromagnetic modes quantized, one can evaluate the spontaneous-emission rate, and explore its variations with the controllable parameters of the system.

The plan of this paper is as follows. In Sec. II we set up the effective-medium formalism for the principal structure, namely, a thin slab region between two semi-infinite one-dimensionally periodic layered structures identified as the photonic crystals and treated within the effective-medium approach. Section III deals with the formalism for the evaluation of the spontaneous-emission rate of a dipole positioned within the central slab region. The results of the theory are given in Sec. IV and are illustrated with reference to typical situations involving a GaAs slab sandwiched between photonic crystals with frequency-independent dielectric functions. Section IV A deals with the situation in which photonic crystal regions have different layer compositions and/or layer thicknesses, leading to different effective uniaxial media, while Sec. IV B concerns a symmetric structure with identical photonic crystal regions. Section V contains comments and conclusions.

II. EFFECTIVE-MEDIUM THEORY OF DIELECTRIC SLAB BETWEEN UNIAXIAL MEDIA

It is well known in electromagnetic theory that in anisotropic media the electromagnetic fields are described by Maxwell equations, with additional constitutive relations that describe the medium [17]:

$$\mathbf{D}=\varepsilon\mathbf{E}, \tag{1}$$

$$\mathbf{B}=\mu\mathbf{H}, \tag{2}$$

where ε and μ are tensors in general. Here we assume electrically anisotropic media, but magnetically isotropic such that μ is the permeability constant and ε is the permittivity tensor. This tensor has nine components in general, but we assume that a principal coordinate system is used such that this tensor is diagonal with only three components ε_x, ε_y, and ε_z along the principal axes of the structure.

Moreover we shall specialize to uniaxial media where $\varepsilon_x=\varepsilon_y=\varepsilon_\parallel$, so that our system has only two principal axes with the z axis as the optic axis. Thus we take the permittivity tensor as

$$\varepsilon=\varepsilon_o\begin{pmatrix}\varepsilon_\parallel & 0 & 0\\ 0 & \varepsilon_\parallel & 0\\ 0 & 0 & \varepsilon_z\end{pmatrix}. \tag{3}$$

The dispersion relations obtained from the Maxwell wave equation of this system lead to two distinct equations [17]

$$k^2=\frac{\omega^2}{c^2}\varepsilon_\parallel \tag{4}$$

for ordinary or TE waves, and

$$k_z^2+\frac{\varepsilon_\parallel}{\varepsilon_z}k_\parallel^2=\frac{\omega^2}{c^2}\varepsilon_\parallel \tag{5}$$

for extraordinary or TM waves that propagate in the medium. For extraordinary waves the magnitude of the wave vector is a function of its direction of propagation, whereas for the ordinary wave it is independent of direction of propagation. These two waves are the two permissible normal modes of the system.

We shall now present the effective-medium approach to the dielectric slab between two photonic crystals. As shown schematically in Fig. 1, our system consists of a dielectric slab occupying the region $0<z<L$, and the photonic crystals occupy the regions $z>L$ and $z<0$. Each photonic crystal consists of a one-dimensionally periodic array of alternating layers of materials. The thicknesses d_1 and d_2 and dielectric functions ε_1 and ε_2 characterize one photonic crystal, while the corresponding parameters for the second photonic crystal are d_3 and d_4 for the thicknesses and ε_3 and ε_4 for the dielectric functions.

In the effective-medium approach each photonic crystal is described by a dielectric tensor of the form given in Eq. (3). In this approach the photonic crystal has the optical characteristic of a uniaxial medium, as described above. The components of the dielectric tensor appropriate for the photonic crystals were given in an illuminating argument in Ref. [12], and it is instructive to summarize the main ideas leading to the effective-medium approach. Consider the average value of the displacement vector $\mathbf{D}_\parallel$ parallel to interfaces over the period (d_a+d_b) of a photonic crystal (with layers labeled a and b) which, by definition, is given by;

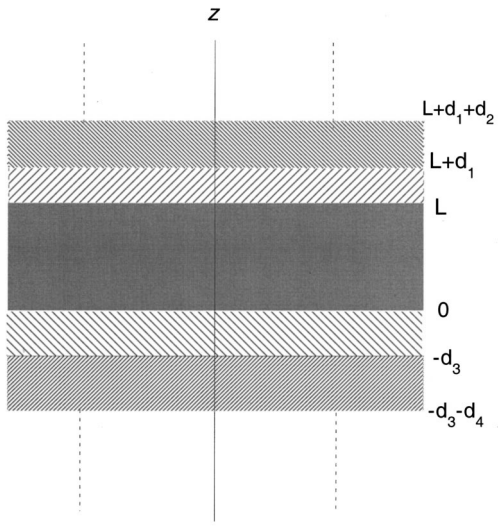

FIG. 1. A schematic representation of the layer system under consideration comprising a thin slab of dielectric function $\varepsilon_s(\omega)$, occupying the region $0<z<L$ between two photonic crystals.

$$\overline{\mathbf{D}}_\parallel=\frac{\varepsilon_a\mathbf{E}_\parallel^{(a)}d_a+\varepsilon_b\mathbf{E}_\parallel^{(b)}d_b}{d_a+d_b}, \tag{6}$$

with the bar denoting the average value. For long-wavelength fields, where the wavelength λ is much greater than d_a and $d_b(\lambda\gg d_a,d_b)$, the variations of the electric field over the crystal period may be neglected, and the electric field may be approximated by its average value over the crystal period. Thus we may write

$$\overline{\mathbf{D}}_\parallel=\varepsilon_\parallel\overline{\mathbf{E}}_\parallel, \tag{7}$$

where

$$\varepsilon_\parallel=\frac{\varepsilon_a d_a+\varepsilon_b d_b}{d_a+d_b}. \tag{8}$$

Similarly the average value of the normal component of the electric field may be written as

$$\overline{E}_z=\left(\frac{D_z^{(a)}}{\varepsilon_a}d_a+\frac{D_z^{(b)}}{\varepsilon_b}d_b\right)\frac{1}{d_a+d_b}. \tag{9}$$

In the long-wavelength approximation the electric displacement may be approximated by its average value over the crystal period, and we write

$$\overline{E}_z=\frac{\overline{D}_z}{\varepsilon_z}, \tag{10}$$

where we now have

$$\varepsilon_z = \varepsilon_a \varepsilon_b \frac{d_a + d_b}{\varepsilon_a d_b + \varepsilon_b d_a}. \tag{11}$$

Equations (8) and (11) are the dielectric tensor components in the effective-medium description. Applying this approach to the pair of photonic crystals at hand, we immediately write the dielectric tensor components for the two semi-infinite crystals as

$$\varepsilon_{\|1} = \frac{\varepsilon_1 d_1 + \varepsilon_2 d_2}{d_1 + d_2}, \tag{12}$$

$$\varepsilon_{z1} = \varepsilon_1 \varepsilon_2 \frac{d_1 + d_2}{\varepsilon_1 d_2 + \varepsilon_2 d_1} \tag{13}$$

for the first photonic crystal, and

$$\varepsilon_{\|2} = \frac{\varepsilon_3 d_3 + \varepsilon_4 d_4}{d_3 + d_4}, \tag{14}$$

$$\varepsilon_{z2} = \varepsilon_3 \varepsilon_4 \frac{d_3 + d_4}{\varepsilon_3 d_4 + \varepsilon_4 d_3} \tag{15}$$

for the second photonic crystal, where the subscripts 1 and 2 on the left-hand sides refer to the first and second photonic crystals, respectively. The dielectric functions of the photonic crystal will be taken to be frequency independent, but the slab dielectric function is assumed to be frequency dependent, and is represented by $\varepsilon_s(\omega)$.

Having determined the forms of the dielectric tensor components we can now investigate the normal modes of the system of the slab between two semi-infinite photonic crystals. The electric fields in the different regions of the slab-crystal structure are determined by applying electromagnetic boundary conditions at $z=0$ and L to the solutions of the wave equation. We write

$$\begin{aligned}
\mathbf{E}(z<0) &= (A_\|, 0, A_z) e^{-ik_{z1}z + i(\mathbf{k}_\| \cdot \mathbf{r}_\| - \omega t)}, \\
\mathbf{E}(z>0) &= (D_\|, 0, D_z) e^{ik_{z2}z + i(\mathbf{k}_\| \cdot \mathbf{r}_\| - \omega t)}, \\
\mathbf{E}(0<z<L) &= [(B_\|, 0, B_z) e^{ik_s z} + (C_\|, 0, C_z) e^{ik_s(z-L)}] \\
&\quad \times e^{i(\mathbf{k}_\| \cdot \mathbf{r}_\| - \omega t)},
\end{aligned} \tag{16}$$

where the A's, B's, C's, and D's are the field amplitudes, $\mathbf{k}_\|$ is the in-plane wave vector parallel to the interface, and k_{zs} and k_{zi} are the wave vectors normal to the interfaces and are given as

$$k_{zs}^2 = \frac{\omega^2}{c^2} \varepsilon_s - k_\|^2, \tag{17a}$$

$$k_{zi}^2 = \frac{\omega^2}{c^2} \varepsilon_{\|i} - \frac{\varepsilon_{\|i}}{\varepsilon_{zi}} k_\|^2 \quad (i=1,2), \tag{17b}$$

which, for notational convenience, we write as k_i $(i=1,2,s)$. The various components of each field amplitude are related to each other by the transversality condition $\nabla \cdot \mathbf{D} = \nabla \cdot (\varepsilon \mathbf{E}) = 0$. Application of electromagnetic boundary conditions at the interfaces $z=0$ and $z=L$ (Fig. 1), and using the transversality condition, leads to the set of equations

$$\begin{aligned}
A_\| - B_\| - C_\| f &= 0, \\
A_\| + B_\| Z_1 - C_\| Z_1 f &= 0, \\
B_\| f + C_\| - D_\| &= 0, \\
B_\| Z_2 f - C_\| Z_2 - D_\| &= 0,
\end{aligned} \tag{18}$$

where

$$Z_i = \frac{\varepsilon_s}{k_s} \frac{k_i}{\varepsilon_{\|i}}, \quad (i=1,2) \quad \text{and} \quad f = e^{ik_s L}. \tag{19}$$

This set of equations admits a nontrivial solution if the determinant vanishes. Setting the determinant equal to zero leads, after simple algebra, to the well-known dispersion relation for the slab between asymmetric structure of two different photonic crystals systems [18–20]:

$$\frac{(k_s/\varepsilon_s) - (k_2/\varepsilon_{\|2})}{(k_s/\varepsilon_s) + (k_2/\varepsilon_{\|2})} f = \frac{(k_s/\varepsilon_s) - (k_1/\varepsilon_{\|1})}{(k_s/\varepsilon_s) + (k_1/\varepsilon_{\|1})} f^{-1}. \tag{20}$$

The dispersion relation in Eq. (20) is for the TM modes. It can be shown that the corresponding relation for the TE modes are obtainable from this by replacing $(\varepsilon_s k_i/\varepsilon_{\|i} k_s)(i=1$ and 2) by (k_s/k_i). In this paper we are concerned with the interface polaritons which are characterized [18,19] by imaginary wave vectors normal to the interfaces such that the waves are decaying with distance from the interfaces at $z=0$ and $z=L$ into the outer regions and are hyperbolic in the slab. These modes are purely extraordinary (or TM) modes. Thus we ignore the TE modes here as they do not contribute to the surface polariton modes. Moreover to see the salient features of the effective medium description we shall ignore retardation effects, which amounts to ignoring throughout (ω/c) terms such as in Eq. (5). In this case dispersion relation (20) for the surface polaritons takes the form

$$\tanh(\beta_s L) = -\frac{\beta_s}{\varepsilon_s} \frac{(\beta_1/\varepsilon_{\|1}) + (\beta_2/\varepsilon_{\|2})}{(\beta_s/\varepsilon_s)^2 + (\beta_1\beta_2/\varepsilon_{\|1}\varepsilon_{\|2})}, \tag{21}$$

where we have made the replacement $\beta_j = ik_j$ $(j=1,2,s)$. This is the general form of the dispersion relation of the system of interest. For illustration purposes we shall consider a specific system in which the slab is GaAs, with a frequency-dependent dielectric function given by

$$\varepsilon_s = \varepsilon_\infty \frac{\omega^2 - \omega_L^2}{\omega^2 - \omega_T^2}, \tag{22}$$

where $\varepsilon_\infty = 10.89$, $\hbar\omega_L = 36.25\,\text{meV}$, and $\hbar\omega_T = 33.29\,\text{meV}$. The photonic crystals parameters are given by the arbitrary set $d_1 = 600\,\text{A}$, $d_2 = 400\,\text{A}$, $\varepsilon_1 = 8.89$, $\varepsilon_2 = 1.3$, $d_3 = 500\,\text{A}$, $d_4 = 300\,\text{A}$, $\varepsilon_3 = 10$, and $\varepsilon_4 = 1.5$.

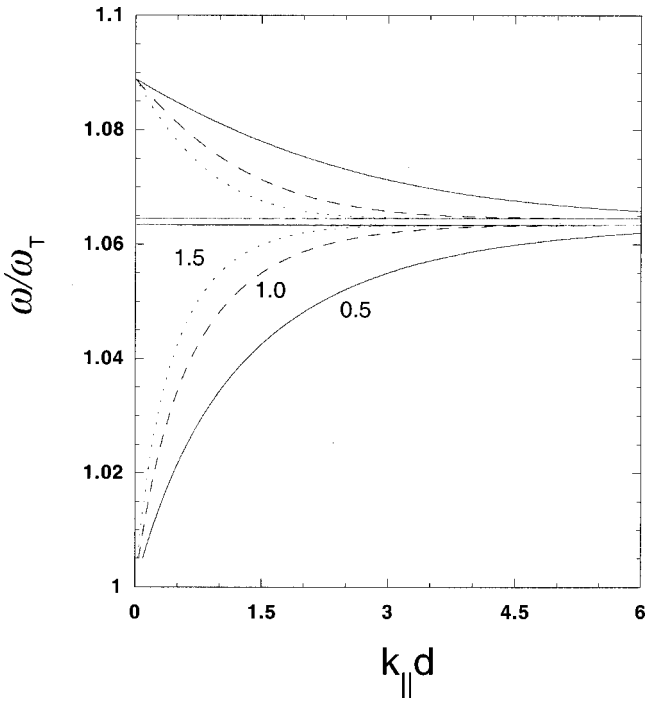

FIG. 2. Dispersion curves of the interface modes in an asymmetric structure. Different pairs of curves correspond to different slab thicknesses $L=0.5d$, d, and $1.5d$, where $d=d_1+d_2$. See main text for other parameters.

The dispersion curves corresponding to Eq. (21) are evaluated numerically for this set of parameters and the results are given in Fig. 2 for different slab thicknesses L, as ω versus the in-plane wave vector $k_\parallel$ parallel to interface, with $d=d_1+d_2$. It is clear that the dispersion curves depend, among other things, on the photonic crystal parameters. In fact by changing the periodicity d of one of the crystals, which is equivalent to changing its dielectric tensor components, the curves are found to shift up or down. The gap that occurs around $\omega=1.064\omega_T$ is the reststrahl region of GaAs, a common feature of band-gap systems which makes them special when one considers the interaction of dipole emitters with these modes, as we shall see in the next sections.

The case of a symmetric structure where the uniaxial media are identical follows immediately from the above discussion by putting $\varepsilon_{\parallel 1}=\varepsilon_{\parallel 2}=\varepsilon_\parallel$, $\varepsilon_{z1}=\varepsilon_{z1}=\varepsilon_z$, and $\beta_1=\beta_2=\beta$. The dispersion relations in this case follow from Eq. (20), and leads to the well known [18,20] even and odd modes:

$$\frac{\varepsilon_s}{\varepsilon_\parallel}\frac{\beta}{\beta_s}=-\tanh\left(\frac{1}{2}\beta_s L\right) \quad \text{(even modes)}, \tag{23}$$

$$\frac{\varepsilon_s}{\varepsilon_\parallel}\frac{\beta}{\beta_s}=-\coth\left(\frac{1}{2}\beta_s L\right) \quad \text{(odd modes)}, \tag{24}$$

These modes are shown in Fig. 3 for different slab thickness. The difference between these two modes and the modes of the asymmetric structure is evident; in the asymmetric structure there is only one mode, and this leads to the interesting feature of the band gap. In the symmetric structure there are two distinct branches; one commences just below ω_L, and the other just above ω_T and there is no gap. For large $k_\parallel$ these two branches approach a single asymptotic value, one from above and the other from below.

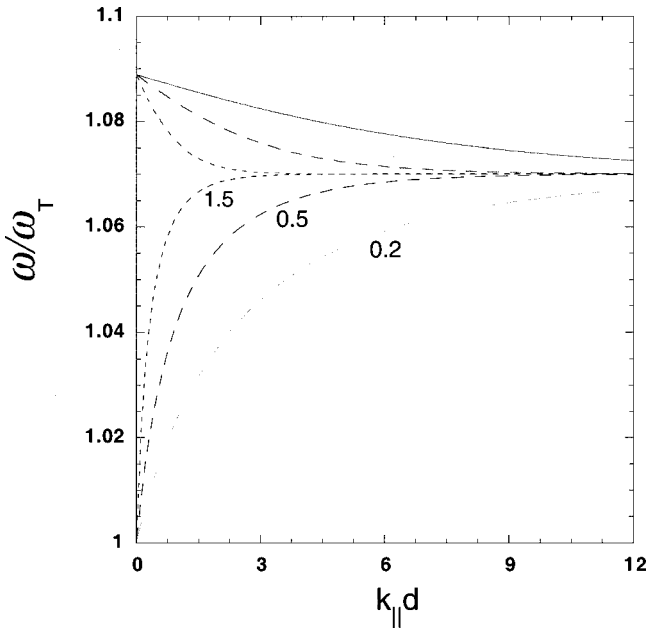

FIG. 3. Dispersion curves for the symmetric structure to be compared with Fig. 2. Note the disappearance of the frequency gap between the horizontal lines in Fig. 2.

III. DIPOLE RELAXATION RATE

Having determined the dielectric tensor components in the effective-medium approach, our next task is the evaluation of the emission rate by dipole emitters whose frequency lies in the frequency range spanned by the interface modes as shown in Figs. 2 and 3. First we have to normalize the modes using standard quantization methods. The quantized electric field is written as sum over the modes λ, in the form

$$\mathbf{E}(\mathbf{r},t)=\int d^2\mathbf{k}_\parallel \sum_\lambda \left[\mathbf{E}_o(\mathbf{k}_\parallel,\lambda)a(\mathbf{k}_\parallel,\lambda)e^{i(\mathbf{k}_\parallel\cdot\mathbf{r}_\parallel-\omega_\lambda t)}+\text{H.c.}\right], \tag{25}$$

where the field function $\mathbf{E}_o$ is determined as follows: first we write the field Hamiltonian of the slab-crystal system as

$$H=H_m+H_s, \tag{26}$$

where H_m is the field Hamiltonian in the anisotropic medium and is given by

$$H_m=\frac{1}{2}\int d^3r[\mathbf{D}\cdot\mathbf{E}+\varepsilon_o c^2 B^2], \tag{27}$$

and H_s is the field Hamiltonian in the slab which, in dispersive media, is given as [32]

$$H_s=\frac{1}{2}\varepsilon_0\int d^3\mathbf{r}\int d^2\mathbf{k}_\parallel\sum_\lambda\left[\frac{\partial}{\partial\omega}(\omega\varepsilon_s)E_\lambda^2+c^2B_\lambda^2\right], \tag{28}$$

where the summation is over all modes, and the dielectric slab can have a frequency-dependent dielectric function. The total Hamiltonain in 26 is now required to reduce to the canonical form

$$H=\frac{1}{2}\sum_{\lambda}\int d^2\mathbf{k}_{\parallel}\hbar\omega(\mathbf{k}_{\parallel},\lambda)[a(\mathbf{k}_{\parallel},\lambda)a^{\dagger}(\mathbf{k}_{\parallel},\lambda)+a^{\dagger}(\mathbf{k}_{\parallel},\lambda)a(\mathbf{k}_{\parallel},\lambda)], \tag{29}$$

where the annihilation and creation operators obey the usual commutation relation, namely

$$[a_i(\mathbf{k}_{\parallel},\lambda),a_j^{\dagger}(\mathbf{k}_{\parallel}',\lambda')]=\delta_{ij}\delta_{\lambda\lambda}\delta(\mathbf{k}_{\parallel}-\mathbf{k}_{\parallel}'). \tag{30}$$

This procedure culminates in the description of the field vector amplitude in terms of some structure functions F and G:

$$\mathbf{E}_o(\mathbf{k}_{\parallel},\lambda)=C(k_{\parallel},\lambda)(\hat{\mathbf{r}}_{\parallel}F_{\lambda}+\hat{z}G_{\lambda}), \tag{31}$$

where the normalization factor $C(k_{\parallel},\lambda)$ is given by

$$C(k_{\parallel},\lambda)=\left(\frac{\hbar\omega_{\lambda}}{(2\pi)^2\varepsilon_o\left[S_E^{\lambda}+\frac{\omega^2}{c^2}S_B^{\lambda}\right]}\right). \tag{32}$$

The form of the structure functions F and G and the normalization factor $C(k_{\parallel},\lambda)$ depend on the particular geometrical structure, and they are given in Sec. IV for symmetric and asymmetric structures separately.

The surface polaritons described by this field will now be coupled to a point oscillating dipole of frequency ω_o that is situated in the slab. The dipole emitter is modeled as a two-level system with the ground $|g\rangle$ state and the excited $|e\rangle$ state separated by transition frequency $\omega_o=(E_e-E_g)/\hbar$. An excited dipole discharges its energy by spontaneously emitting a surface polariton. For a dipole emitter situated at $\mathbf{r}=(\mathbf{0},z)$ within the slab, the relaxation rate is given by Fermi's golden rule as

$$\Gamma(\mathbf{r})=\frac{2\pi}{\hbar}\sum_{\lambda}\int d^2\mathbf{k}_{\parallel}|\langle e,\{0\}|H_{\mathrm{int}}|g,\{k_{\parallel},\lambda\}\rangle|^2\times\delta(\hbar(\omega_o-\omega(k_{\parallel},\lambda)), \tag{33}$$

where H_{int} is the electric dipole interaction Hamiltonian [21,22]

$$H_{\mathrm{int}}=-\frac{\boldsymbol{\mu}\cdot\mathbf{D}(\mathbf{r})}{\varepsilon(\mathbf{r})}, \tag{34}$$

with $\mathbf{D}(\mathbf{r})=\varepsilon(\mathbf{r})\,\mathbf{E}(\mathbf{r})$ is the electric displacement field at the position of the point dipole inside the dielectric slab where the permittivity is $\varepsilon(\mathbf{r})=\varepsilon_o\varepsilon_s$, and $\boldsymbol{\mu}$ is the dipole moment vector, which we write as $\boldsymbol{\mu}=\mu_{\parallel}\hat{\mathbf{r}}_{\parallel}+\mu_z\hat{z}$. Expressions (25), (33), and (34) lead, after carrying out the $k_{\parallel}$ integration, to the following expression for the atomic dipole relaxation rate:

$$\Gamma_{\lambda}(\mathbf{r})=\Gamma_{\parallel}+\Gamma_z=\left(\frac{2\pi\mu}{\hbar}\right)^2\frac{k_{\lambda}|C(k_{\lambda})|^2}{|(\partial\omega/\partial k_{\parallel})|_{k_{\lambda}}}\left[\frac{1}{2}\frac{\langle\mu_{\parallel}\rangle^2}{\mu^2}F_{\lambda}^2+\frac{\langle\mu_z\rangle^2}{\mu^2}G_{\lambda}^2\right], \tag{35}$$

where k_{λ} is the value of $k_{\parallel}$ at which a horizontal line at $\omega=\omega_o$ crosses the dispersion curve labeled λ.

The final step in the derivation of the spontaneous-emission rate is to incorporate the local-field corrections which account for the fact that the dipole interacts with its own local field, rather than the macroscopic field which we have derived here assuming locally continuous media. This matter received attention in the recent literature [23–25], and it is generally accepted that such effects lead to modifications of the spontaneous rate, which can be written as

$$\Gamma_{\lambda}(\mathbf{r})\rightarrow\Gamma_{\lambda}(\mathbf{r})R(\varepsilon_s), \tag{36}$$

where $R(\varepsilon_s)$ is the local-field correction factor. This factor is, in general, model dependent, relying on a consideration of small virtual free-space cavity surrounding the point dipole, and is embedded in the continuous medium where the dipole is situated [26]. However, there has been a number of experiments [26–28] to investigate the model dependence of the local fields. These experiments favor the virtual cavity model due to Glauber and Lewenstein [23]. We shall therefore adopt the Glauber-Lewenstein scheme according to which the local field correction factor is given as

$$R_{\mathrm{GL}}[\varepsilon_s(\omega_o)]=\left(\frac{3\varepsilon_s(\omega_o)}{2\varepsilon_s(\omega_o)+1}\right)^2 \tag{37}$$

with $\varepsilon_s(\omega_o)$ the local dielectric function of the slab calculated at the dipole transition frequency. An alternative to the above procedure for incorporating local-field effects into the theory is to use an interaction Hamiltonain in which the dipole couples to the local microscopic displacement field rather than the macroscopic one [29,30]. Expressions (35) and (37) will be calculated numerically in Sec. IV, in the nonretarded limit, subject to the condition that ω and $k_{\parallel}$ satisfy the dispersion relation (21) for asymmetric structures or Eqs. (23) and (24) for symmetric ones.

IV. NUMERICAL RESULTS

The spontaneous emission rate is now given by Eqs. (35)–(37), with local-field effects included. To perform the numerical calculation of the decay rate we need to specify the field amplitude and the functions F and G. These depend on the structure geometry, and we in Secs. IV A and IV B consider both asymmetric and symmetric structures.

A. Asymmetric structure

For the asymmetric structure case in which the slab is sandwiched between two different photonic crystals, the field function of mode λ is given by Eqs. (25), (31), and (32), with

$$S_E=\frac{\varepsilon_{\|1}}{2\beta_1}\left(1+\frac{\varepsilon_{\|1}}{\varepsilon_{z1}}\frac{k_\|^2}{\beta_1^2}\right)+\frac{\varepsilon_{\|2}}{2\beta_2}\left(1+\frac{\varepsilon_{\|2}}{\varepsilon_{z2}}\frac{k_\|^2}{\beta_2^2}\right)R^2+\frac{\partial}{\partial\omega}(\omega\varepsilon_s)$$
$$\times\left[(M^2+N^2)\frac{\beta_s^2+k_\|^2}{\beta_s^2}\frac{\sinh(\beta_s L)}{\beta_s L}+2MN\frac{\beta_s^2-k_\|^2}{\beta_s^2}\right]$$
$$\times e^{-\beta_s L}L, \tag{38}$$

and

$$S_B=\frac{\varepsilon_{\|1}^2}{2\beta_1^3}+\frac{\varepsilon_{\|2}^2}{2\beta_2^3}+\frac{\varepsilon_s^2}{\beta_s^2}\left[(M^2+N^2)\frac{\sinh(\beta_s L)}{\beta_s L}-2MN\right]$$
$$\times e^{-\beta_s L}L, \tag{39}$$

$$M=-\frac{1}{2}\frac{1-y_1}{y_1}, \tag{40}$$

$$N=-M\frac{1-y_2}{1+y_2}f, \tag{41}$$

$$R=2M\frac{y_2}{1+y_2}f, \tag{42}$$

$$y_i=\frac{\varepsilon_s}{\beta_s}\frac{\beta_i}{\varepsilon_{\|i}}, \quad (i=1,2), \tag{43}$$

$$f=\exp(-\beta_s L). \tag{44}$$

The structure functions that appear in Eq. (3) can be specified in all three regions. However, since we are only interested here in the region within the slab where this approach is valid, we need only display the structure functions for a dipole positioned at $\mathbf{r}=(\mathbf{0},z)$, where $0<z<L$:

$$F_\lambda=[Me^{-\beta_s z}+Ne^{\beta_s(z-L)}]_\lambda, \tag{45}$$

$$G_\lambda=\left[i\frac{k_\|}{\beta_s}(Me^{-\beta_s z}-Ne^{\beta_s(z-L)})\right]_\lambda. \tag{46}$$

It should be noted here that Eqs. (38)–(46) are given for the general case where retardation effects are included, but here we are only interested in the nonretarded limit, and the numerical calculations will be done for this case. Having specified the various field amplitude parameters, we now present the results of our numerical analysis and the results of the calculations are given Figs. 4–7 as the dipole relaxation rate Γ, in units of $\Gamma_s=\omega_T=5.057\times10^{13}\,\mathrm{s}^{-1}$.

Figure 4 displays the relaxation rate as a function of the dipole transition frequency ω_o/ω_T in the reststrahl region of GaAs for a dipole oriented parallel (solid curve) and normal (dashed curve) to the interfaces. A characteristic feature of the frequency dependence is the divergence of the rate as the frequency approaches one of the asymptotic values noted in Figs. 2 and 3. This can be traced to the fact that the group-velocity approaches zero in this limit. This behavior is well known in the literature [31,32] where the rate suffers suppression when the dipole transition frequency is within the

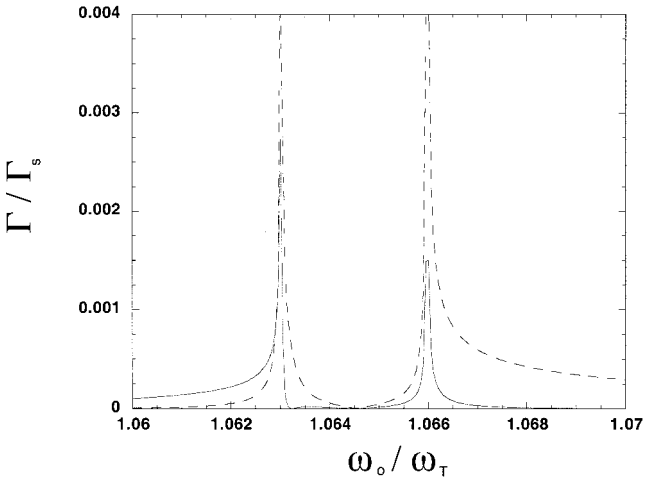

FIG. 4. Dipole relaxation rate in units of $\Gamma_s=\omega_T$, as a function of dipole transition frequency for a dipole emitter positioned at $z=d/4$ and for $L=d/2$ with $d=d_1+d_2$. The solid curve is the parallel rate, and the dashed one is the perpendicular rate. See the main text for the other parameters used here.

reststrahl region. Near the band edges the group velocity approaches zero, and the rate peaks at the edge sides of the gap. In Figs. 5(a) and 5(b) we display the rate as a function of the slab thickness L/d for dipole located at $z=d/4$ with transition frequency (a) $\omega_o=1.066\omega_T$ and (b) $\omega_o=1.062\omega_T$. The solid curve is the parallel rate, while the dotted curve is the normal rate. For a small slab thickness the rate diverges, consistent with the interaction with interface modes. For large slab thickness the dipole rates diminish to zero, since the interface modes themselves vanish in this limit. For certain values of slab thickness the dipole rate is totally suppressed in a manner that depends on the dipole orientation and frequency. For frequencies above the band gap the parallel rate for a dipole at the given fixed position vanishes at a certain slab width L, while the normal rate shows no such behavior. At frequencies below the gap the situation is reversed, and it is the normal rate that vanishes at a certain L. For frequencies within the gap, both rates vanish. This is an interesting result, since it suggests that by appropriate choice of geometrical arrangement it is possible to control the atomic radiation rate in the cavity and may use the cavity as filter to suppress or enhance the desired component of the relaxation rate. Figures 6(a) and 6(b) show the relaxation rate as a function of dipole position z/d for slab thickness $L=d/2$, for dipole transition frequencies (a) $\omega_o=1.066\omega_T$ and (b) $\omega_o=1.062\omega_T$. The solid lines correspond to the parallel rate, and the dashed lines to the normal rate. Clearly, since the geometrical structure of interest is not symmetric, the rate is not symmetric with respect to the slab center.

B. Symmetric structure

The field functions for the symmetric case are easily obtained from the asymmetric case by putting $\varepsilon_{\|1}=\varepsilon_{\|2}=\varepsilon_\|$, $\varepsilon_{z1}=\varepsilon_{z2}=\varepsilon_z$, $d_1=d_3$, $d_2=d_4$, and $\beta_1=\beta_2=\beta$. In this case expressions (38)–(44) reduce to the following equations appropriate for the symmetric structure:

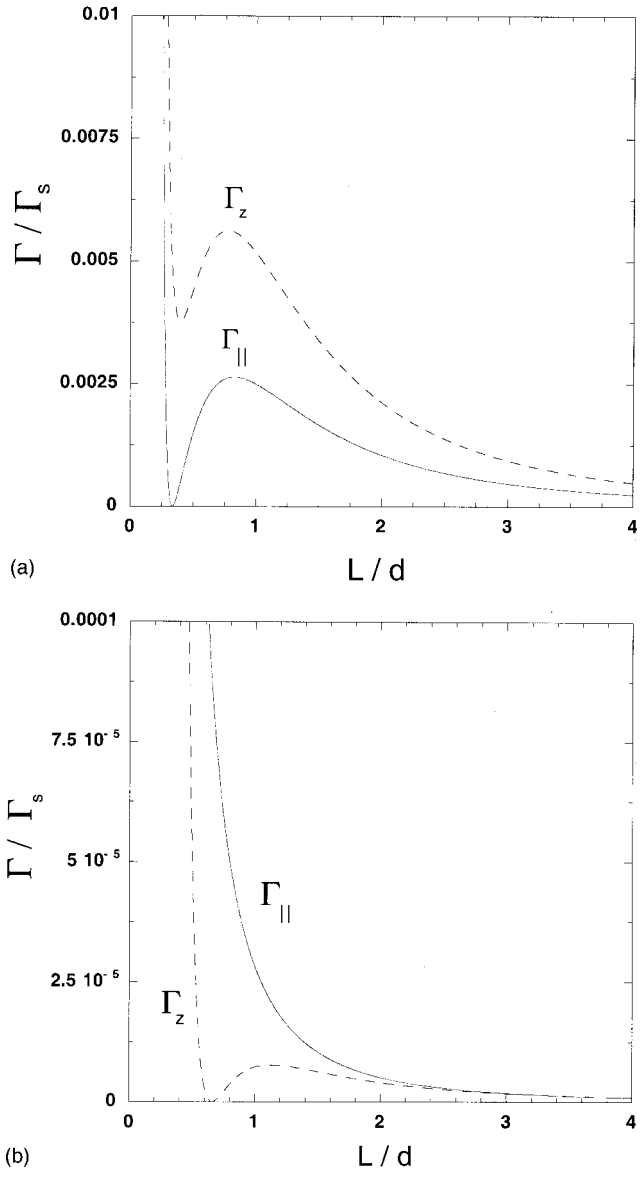

FIG. 5. Dipole relaxation rates $\Gamma_{\|}$ and Γ_z, in units of $\Gamma_s = \omega_T$, against the slab thickness for a dipole emitter at $z = d/4$, (a) $\omega_o = 1.066\omega_T$ and (b) $\omega_o = 1.062\omega_T$. See the main text for other parameters.

$$S_E = \frac{\varepsilon_{\|}}{\beta}\left(1 + \frac{\varepsilon_{\|}}{\varepsilon_z}\frac{k_{\|}^2}{\beta^2}\right) + \frac{\partial}{\partial\omega}(\omega\varepsilon_s)(2M^2L) \times\left[\frac{\beta_s^2 + k_{\|}^2}{\beta_s^2}\frac{\sinh(\beta_s L)}{\beta_s L} + \alpha\frac{\beta_s^2 - k_{\|}^2}{\beta_s^2}\right]e^{-\beta_s L}, \quad (47)$$

$$S_B = \frac{\varepsilon_{\|}^2}{\beta^3} + \frac{\varepsilon_s^2}{\beta_s^2}(2M^2L)\left[\frac{\sinh(\beta_s L)}{\beta_s L} + \alpha\right]e^{-\beta_s L}, \quad (48)$$

where

$$M = -\frac{1}{2}\frac{1-y}{y}, \quad (49)$$

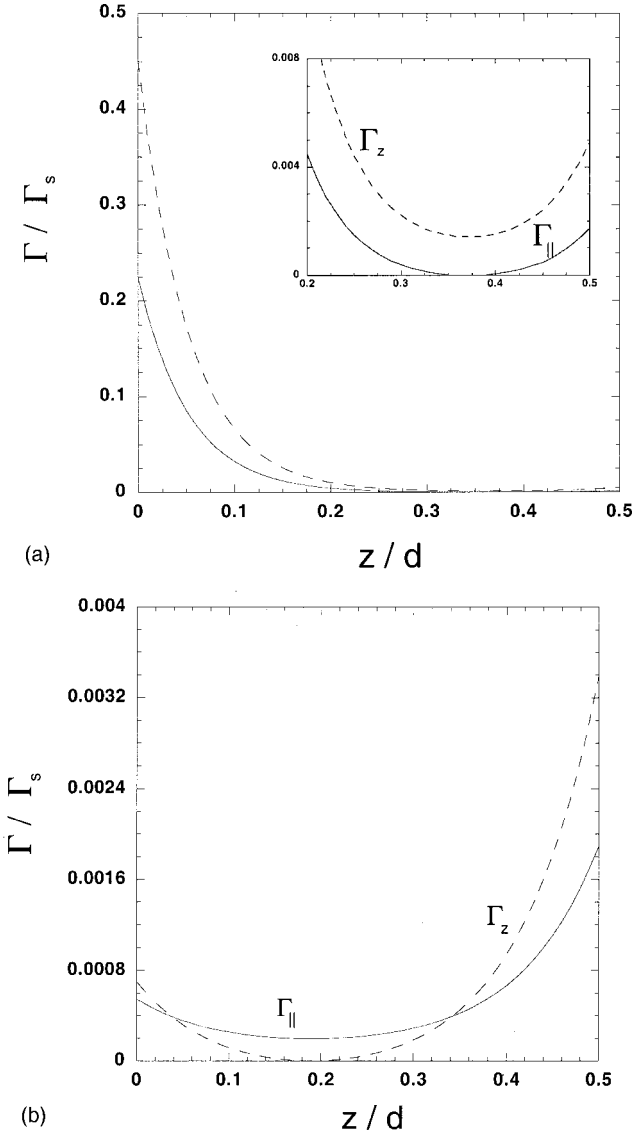

FIG. 6. Dipole relaxation rates $\Gamma_{\|}$ and Γ_z, in units of $\Gamma_s = \omega_T$, in the case of the asymmetric structure against the dipole position z/d for a slab thickness $L = d/2$ and transition frequencies (a) $\omega_o = 1.066\omega_T$ and (b) $\omega_o = 1.062\omega_T$.

$$N = \alpha\frac{1}{2}\frac{1-y}{y}, \quad (50)$$

$$y = \frac{\varepsilon_s}{\beta_s}\frac{\beta}{\varepsilon_{\|}}, \quad (51)$$

$$f = \exp(-\beta_s L), \quad (52)$$

where $\alpha = 1$ for the even mode and -1 for odd mode, which have been given in Eqs. (23) and (24). The structure functions F and G are still given by Eqs. (45) and (46) but with M and N as in Eqs. (49) and (50).

As in asymmetric geometry, the even and odd modes of this structure constitute relaxation channels for the atomic dipole and the relaxation rate in this case can be calculated from expressions (35)–(37). The results are given in Figs.

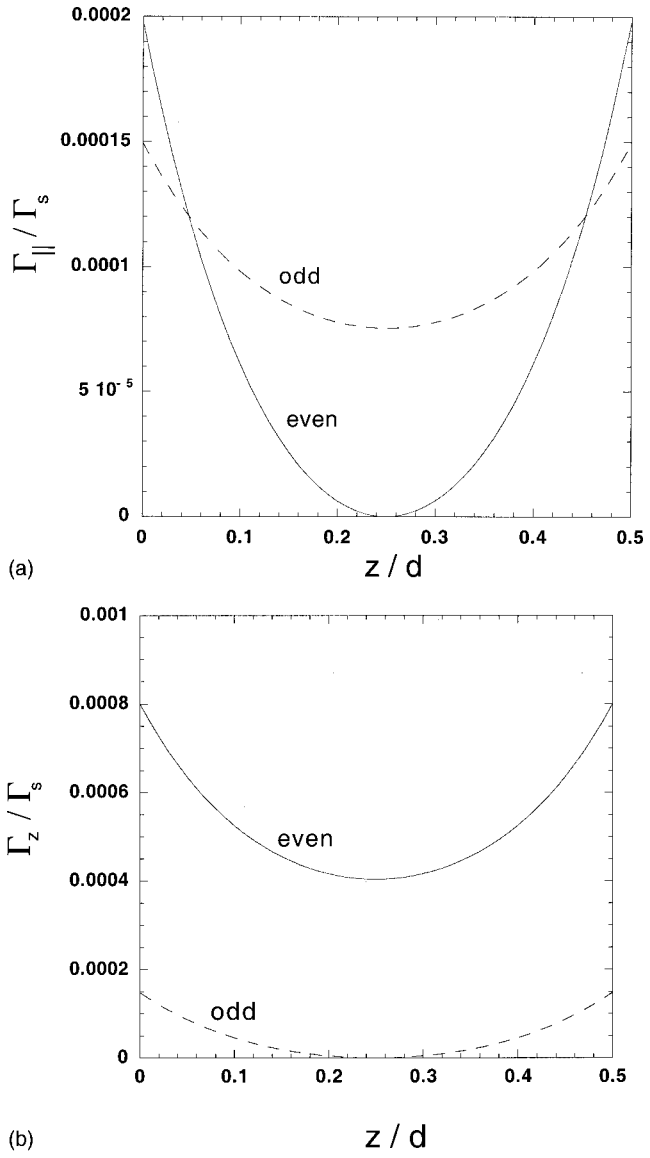

FIG. 7. Dipole relaxation rates $\Gamma_{\|}$ and Γ_z, in units of $\Gamma_s = \omega_T$, for the symmetric structure against the dipole position for a fixed slab thickness $L = d/2$: (a) the parallel rate, and (b) the normal rate. The curves were calculated for the same in-plane wave vector $k_{\|}d = 3.5$, which corresponds to transition frequency ($\omega_o = 1.0764\omega_T$) in the even branch (full curve) and to ($\omega_o = 1.0672\omega_T$) in the odd branch (dashed curve).

7(a) and 7(b) as the rate Γ, in units of $\Gamma_s = \omega_T = 5.057 \times 10^{13}\,\mathrm{s}^{-1}$. Figures 7(a) and 7(b) show Γ as a function of dipole position for $L = d/2$. The decay rate is symmetric with respect to the slab midpoint $L/2$. This is to be contrasted with the asymmetric case. At the slab midpoint both the parallel decay rate that couples to the even mode and the normal decay rate that couples to the odd mode are zero, while other rates are finite.

V. DISCUSSION AND CONCLUSIONS

In this paper we have focused on the application of the effective-medium theory to the problem of spontaneous emission in a nanoscale dielectric cavity QED situation. The effective medium approach permits a system of one-dimensionally periodic layered structure (photonic crystal) to be represented as a uniaxial medium with well-defined dielectric tensor components. We have shown how this leads to a determination of the electromagnetic fields localized within a slab which is sandwiched between two such photonic crystals, and hence to the evaluation of the decay rate of the dipole emitter situated in the slab region. We have illustrated the theory for dipole emitters with frequencies in the reststrahl band of GaAs, with the dipole situated within a GaAs slab which is sandwiched between two sets of photonic crystals of given layer widths and compositions. When compared with typically numerically intensive methods that would normally be needed to solve such a problem, the effective-medium approach is considerably more convenient for the evaluation of spontaneous emission in this and other complicated dielectric cavity QED contexts involving one or more sets of one-dimensionally periodic layers.

The results point to a number of interesting features, which arise from the variation of the adjustable parameters of the system, namely, the dipole oscillation frequency, dipole vector orientation, dipole position within the slab, the slab width, and finally, the photonic crystal parameters: layer widths and dielectric functions. We have shown that the dipole rate spans a wide range of values for dipole relaxation into the interfacelike modes of the structure. These modes propagate along the interfaces, but are localized within the slab region, and decay exponentially into the photonic crystal regions. We have seen that these modes and their coupling to dipole emitters positioned within the slab are sensitive to the values of the parameters mentioned above, constituting potential flexibility for tailoring such a structure as, for example, for the purpose of achieving a desired suppression of the spontaneous rate. One feature that should be highlighted in this context is the appearance of a frequency gap between the pair of interface dispersion curves. This gap is present only when the two photonic crystal regions are different, and disappears when they are identical. A second feature of the asymmetric case is that for a given emitter position there exists a slab width in which the point dipole would not decay spontaneously.

The effective-medium approach can in fact be applied to situations in which all three regions of the structure possess frequency-dependent dielectric functions. A particular case is that in which one or both photonic crystals has a metallic component. This situation is likely to be considerably more involved algebraically than the case considered here, but should still benefit from the simplifications afforded by the effective-medium picture. This problem will not be pursued any further here.

ACKNOWLEDGMENTS

The authors are grateful to Rodney Loudon, David Andrews, Bryan Dalton, Joe Eberly, and Roy Glauber for useful discussions. A.K. would like to thank Joe Eberly for hospitality while at the Rochester Theory Center for Optical Science and Engineering.

[1] E. M. Purcell, Phys. Rev. **69**, 681 (1946).
[2] E. Hinds, in *Cavity Quantum Electrodynamics*, edited by P. Berman (Academic, New York, 1994).
[3] H. Khosravi and R. Loudon, Proc. R. Soc. London, Ser. A **436**, 373 (1992).
[4] S. M. Dutra and P. L. Knight, Phys. Rev. A **53**, 3587 (1996).
[5] H. P. Urbach and G. J. A. Rikken, Phys. Rev. A **57**, 3913 (1996).
[6] S. Alawfi and M. Babiker, Phys. Rev. A **58**, 1 (1998).
[7] R. A. Depine and M. L. Gigli, Phys. Rev. B **49**, 8437 (1994).
[8] M. L. Gigli and R. A. Depine, Opt. Express **1**, 250 (1997).
[9] H. K. Shin, I. Kim, E. J. Kim, J. H. Kim, E. K. Lee, M. K. Lee, J. K. Mun, C. S. Park, and Y. S. Yi, Jpn. J. Appl. Phys. **35**, 506 (1990).
[10] H. Soda, K. Iga, C. Kitahara, and Y. Suematsu, Jpn. J. Appl. Phys. **18**, 2329 (1979).
[11] M. Ogura, T. Hata, N. J. Kawai, and T. Yao, Jpn. J. Appl. Phys. **22**, L112 (1983).
[12] V. M. Agranovich and V. E. Kravtsov, Solid State Commun. **55**, 85 (1985).
[13] N. Raj and D. R. Tilley, Solid State Commun. **55**, 373 (1985).
[14] N. Raj and D. R. Tilley, Phys. Rev. B **36**, 7003 (1987).
[15] T. Dumelow and D. R. Tilley, J. Opt. Soc. Am. A **100**, 633 (1993).
[16] G. Borstel and H. J. Falge, Appl. Phys. **16**, 211 (1978).
[17] J. A. Kong, *Theory of Electromagnetic Waves* (Wiley, New York, 1975).
[18] M. Cottam and D. R. Tilley, *Introduction to Surface and Superlattice Excitations* (Cambridge University Press, Cambridge, England, 1989).
[19] V. M. Agranovich and D. L. Mills, *Surface Polaritons* (North-Holland, Amsterdam, 1982).
[20] M. Babiker, N. C. Constantinou, and B. K. Ridley, Phys. Rev. B **48**, 2235 (1993).
[21] B. J. Dalton and M. Babiker, Phys. Rev. A **56**, 905 (1997); M. Babiker and R. Loudon, Proc. R. Soc. London, Ser. A **385**, 439 (1983).
[22] C. Cohen-Tannouji, J. Dupont-Roc, and G. Grynberg, *Photons and Atoms: Introduction to Quantum Electrodynamics* (Wiley, New York, 1997).
[23] R. J. Glauber and M. Lewenstein, Phys. Rev. A **43**, 467 (1991).
[24] S. M. Barnett, B. Hutner, R. Loudon, and R. Matloob, J. Phys. B **29**, 3763 (1996).
[25] S. M. Barnett, in *Quantum Fluctuations*, Les Houches Session No. LXIII, edited by S. Reynaud, E. Giacobino, and J. Zinn-Justin (Elsevier, Amsterdam, 1997).
[26] G. L. J. A. Rikkin and Y. A. R. R. Kessener, Phys. Rev. Lett. **74**, 880 (1995).
[27] F. J. P. Schuurmans, D. T. N. de Lang, G. H. Wegdam, R. Spike, and Ad Lagendijk, Phys. Rev. Lett. **80**, 5077 (1998).
[28] P. de Vries and Ad Lagendijk, Phys. Rev. Lett. **81**, 1381 (1998).
[29] G. Juzeliunas, Chem. Phys. **198**, 145 (1995).
[30] G. Juzeliunas, Phys. Rev. A **53**, 3543 (1996).
[31] S. John and J. Wang, Phys. Rev. B **43**, 12 772 (1991).
[32] A. Kamli, M. Babiker, A. Al-Hajry, and N. Enfati, Phys. Rev. A **55**, 1454 (1997).